



# HHS Public Access

Author manuscript

*Colloids Surf B Biointerfaces*. Author manuscript; available in PMC 2017 November 29.

Published in final edited form as:

*Colloids Surf B Biointerfaces*. 2015 October 01; 134: 370–376. doi:10.1016/j.colsurfb.2015.07.014.

## Bacteria and Osteoblast Adhesion to Chitosan Immobilized Titanium Surface: A Race for the Surface

Berit L. Foss<sup>a</sup>, Niranjan Ghimire<sup>a</sup>, Ruogu Tang<sup>b</sup>, Yuyu Sun<sup>b,\*</sup>, and Ying Deng<sup>a,\*</sup>

<sup>a</sup>Department of Biomedical Engineering, University of South Dakota, 4800 North Career Avenue, Sioux Falls, South Dakota 57107, USA

<sup>b</sup>Department of Chemistry, The University of Massachusetts, One University Avenue, Lowell, MA 01854, USA

### Abstract

In order to evaluate the anti-infective efficacy of the titanium implant materials, two co-culture systems, a low-bacteria/osteoblast (L-B) and a high-bacteria/osteoblast system (H-B), were established. Untreated (UN-Ti), sulfuric acid-treated (SA-Ti), and chitosan immobilized titanium (SA-CS-Ti) materials were developed and evaluated. Bacteria and osteoblast behaviors, including initial attachment (evaluated at 30 minutes), adhesion (evaluated at 4 hours), and osteoblast spreading on each material surface were evaluated using quantification assays, scanning electron microscopy (SEM), and confocal microscopy. Quantification analysis at 30 minutes showed significantly higher number of osteoblast present on SA-CS-Ti in both L-B ( $10,083 \pm 2,626$ ) and H-B ( $23,592 \pm 2,233$ ) than those on the UN-Ti ( $p < 0.05$ ). SEM observation and confocal microscopy results showed more surface area was occupied by adhered osteoblasts on SA-CS-Ti than UN-Ti and SA-Ti in both co-culture systems at 30 minutes. At all time points, SA-CS-Ti had the lowest level of bacterial adhesion compared to UN-Ti and SA-Ti in both co-culture systems. A significantly ( $p < 0.05$ ) lower number of bacteria were recovered from SA-CS-Ti ( $2,233 \pm 681$ ) in the H-B system compared to UN-Ti ( $5,367 \pm 1,662$ ) and SA-Ti ( $4,533 \pm 680$ ) at 4 hours. Quantitative and qualitative co-culture results show the great potential of chitosan immobilization onto implant materials to prevent implant-associated infections.

### Keywords

Anti-infective; co-culture; osteoblast; implant; chitosan immobilized titanium

### Introduction

The design of orthopedic implants has focused on the biocompatibility, structural functions, and mechanical properties of the implant. Titanium (Ti) has been a major breakthrough for

\*Corresponding Authors, Professor Ying Deng, Ph.D., Tel: (+1) 605-367-7775, Fax: (+1) 605-367-7836, Ying.Deng@usd.edu, Professor Yuyu Sun, PhD, Tel: 978-934-3637, Fax: 978-934-3013, yuyu\_sun@uml.edu.

**Publisher's Disclaimer:** This is a PDF file of an unedited manuscript that has been accepted for publication. As a service to our customers we are providing this early version of the manuscript. The manuscript will undergo copyediting, typesetting, and review of the resulting proof before it is published in its final citable form. Please note that during the production process errors may be discovered which could affect the content, and all legal disclaimers that apply to the journal pertain.

use in such implants due to its good mechanical strength and osseointegration properties[1–3]. Recently, numerous surface modification techniques, such as biological coatings and acid and alkali etching, have been widely researched for Ti-based orthopedic implants to further encourage bioactivity and osseointegration[4–8]. These modifications modulate the surrounding biological environment of osteoblasts in order to increase protein and cellular adhesion with a goal to facilitate osseointegration. Current *in vitro* and *in vivo* research has shown that an increase in Ti surface roughness increases osteoblast adhesion which is key for osseointegration [1, 7, 9, 10]. However, surface modifications to mitigate possible adverse tissue responses, especially infection, have not been well established.

Patients undergoing implantation surgery are treated with systemic antibiotics, although their efficacy is limited when a biofilm is established on the implant surface [11]. As the World Health Organization [12] has reported in 2014, high rates of antibiotic resistance have been observed in all WHO regions in common bacteria, such as *Escherichia coli* and *Staphylococcus aureus*, causing common nosocomial and community-acquired infections [12]. Because initial adhesion of bacteria to a biomaterial surface is believed to be an important event in the pathogenesis of biofilm-associated infection, various approaches have been tried to modify titanium surfaces to minimize bacterial adhesion [13] and interfere with the microbial colonization process [14, 15].

Roughened titanium implant surfaces have been shown to encourage osseointegration properties at the cellular level, such as osteoblast attachment, adhesion, spreading, and proliferation [16]. A consequence of increased titanium surface roughness, shown in the literature [10, 14, 17], as well as in our study, is that the bacteria attachment rate also increases - leading to a higher risk for infection. In order to prepare for this “post-antibiotic era – in which common infections and minor injuries can kill,” [12] we immobilized chitosan onto rough Ti material to prevent infections related to orthopedic implants. The chitosan modification has shown to increase osseointegration of titanium implant material and minimize bacterial attachment in conventional *in vitro* evaluation systems (signal bacteria or osteoblast culture) [18].

The fate of a biomaterial implant has been hypothesized as a “race for the surface” between bacterial and osteoblast adhesion [19]. This hypothesis aids researchers in the exploration for further surface modification as a means to improve osseointegration and the clinical outcome of orthopedic surgeries [2, 14]. Our previous research has combined two surface modifying techniques, sulfuric acid treatment and chitosan immobilization, to address poor osseointegration and implant-related infection, simultaneously [18]. We hypothesize that the increased surface roughness caused by the sulfuric acid treatment will increase osteoblast attachment, while the immobilized chitosan will decrease bacteria attachment. To further test the hypothesis, in this study, we developed two osteoblast/bacteria co-culture systems to evaluate the race for the surface behavior of osteoblast and bacteria towards the unmodified and the modified Ti materials. Osteoblasts and *Staphylococcus aureus*, a bacteria commonly found in implant-related infections[12, 15, 20, 21], were employed to set up the two osteoblast/bacteria co-culture systems to investigate the behavior of osteoblast and bacteria to Ti surfaces simultaneously. Using the co-culture systems we have investigated the

interaction between osteoblast and *S. aureus* in a “race for the surface” scenario and demonstrated the chitosan surface modification aids the osteoblasts to win this race.

## Materials and Methods

### Materials and reagents

The materials and reagents used in this study are from Sigma unless otherwise noted: Dulbecco’s Phosphate Buffered Saline (PBS), fetal bovine serum, trypan blue, fluorescein diacetate (FDA), propidium iodide (PI), acetone, absolute ethanol, 25% glutaraldehyde, titanium foil (purity: 99.7%; 0.25 mm in thickness), dopamine hydrochloride, glutaraldehyde (25%), and chitosan with low molecular weight (75–85% deacetylated; viscosity: 20–300 cP, 1 wt.% in 1% acetic acid at 25°C; the molecular weight is approximately 50,000–190,000 daltons based on viscosity) were purchased from Sigma-Aldrich. Osteoblast-like cells, SaOS-2 (ATCC HTB-85) and *S. aureus* (ATCC 6538) were purchased from American Type Culture Collection. Dulbecco’s Modified Eagle Medium (DMEM), non-essential amino acids, and antibiotics were purchased from Fisher Scientific.

### Titanium Surface Modifications

Titanium samples were prepared and characterized as previously described [18]. To prepare the titanium samples, the Ti foil was cut into 1×1 cm<sup>2</sup> and ultrasonically cleaned with acetone, ethanol, and lastly, deionized water. The resulting unmodified samples are referred to as UN-Ti. The Ti samples were then treated in 48% H<sub>2</sub>SO<sub>4</sub> at 60°C under continuous stirring for 3 hours. These samples were washed with distilled water and dried under vacuum. These samples were designated as SA-Ti, the intermediate product of the chitosan modification. For the preparation of the chitosan immobilized Ti (SA-CS-Ti) in which the chitosan is covalently grafted on to the Ti surface, the SA-Ti samples were treated with 5 mg/mL dopamine hydrochloride in a 10% 0.1 M Tris–HCl aqueous solution at room temperature for 12 hours. This was followed by immersion in 3% glutaraldehyde at 4°C overnight. Afterwards, the samples were immersed in 0.5% chitosan solution (in 1% acetic acid aqueous solution) at room temperature for 18 hours, rinsed with distilled water, and dried under a vacuum. Surface modifications were confirmed through X-ray photoelectron spectroscopy (XPS) analysis.

### Osteoblast Cell Culture

Osteoblasts were thawed and cultured at a density of 5,000 cells/cm<sup>2</sup>. The osteoblasts were incubated at 37°C at 5% CO<sub>2</sub> in culture media of DMEM/High Glucose medium containing 1% non-essential amino acids, 1% antibiotics, and 10% fetal bovine serum. The medium was changed the next day and then every three days until confluency reached 90%. Osteoblasts were then collected using 0.05% trypsin with EDTA. Osteoblasts were quantified using trypan blue and a hemocytometer.

### Bacteria Culture

*Staphylococcus aureus* (*S. aureus*) was cultured in tryptic soy broth (TSB) for 18 hours at 37°C. The bacteria were centrifuged at 5,000 rpm for 5 minutes. The supernatant was removed and the bacteria pellet was gently washed with PBS (×3). The pellet was

resuspended in PBS and serial dilutions were used to obtain specific bacteria concentrations. Bacteria concentration was determined through agar plate spreading.

### **Co-Culture System Establishment**

Titanium samples (UN-Ti, SA-Ti, and CS-SA-Ti) were placed into previously labeled wells of 24 well non-tissue culture plates. Suspended osteoblast cells (100,000/sample) and bacteria (L-B: 10,000/sample or H-B: 100,000/sample) were seeded to their respective wells simultaneously and suspended in a modified medium (98% DMEM w/10% FBS and 2% Tryptic Soy Broth) for a total volume of 500  $\mu$ L. The co-cultures were incubated at 37°C in 5% CO<sub>2</sub> for time points determined (at 30 minutes to study initial attachment and at 4 hours to study steady-state adhesion). At each time point, modified medium was removed and samples were collected for the following quantitative and qualitative assays.

### **Scanning Electron Microscopy Preparation**

UN-Ti, SA-Ti, and SA-CS-Ti samples were prepared in co-culture conditions as described in the co-culture system establishment section. At each time point, samples were collected for SEM observation. The samples were fixed with 2.5% glutaraldehyde in PBS, dehydrated using a series of ascending ethanol concentrations (70%, 80%, 90% and 100% at 5 minutes each), air-dried at 4°C for 24 hours, and sputter-coated (Cressington Scientific) with gold at a thickness of 14–15 nm. The samples were then observed and imaged using a scanning electron microscope (Quanta 450 SEM, FEI).

### **Confocal microscope preparation and observation**

Overnight-grown bacteria were collected, washed, and fluorescent stained with FDA at a concentration of 1 mg FDA per 10<sup>6</sup> bacteria. The FDA-stained bacteria were then used for the co-culture with the osteoblasts as described in the co-culture system establishment section. At each time point (30 minutes and 4 hours), samples were washed with assay medium (DMEM without antibiotics) and were fixed with 2.5% glutaraldehyde in PBS for 15 minutes, followed by a PBS wash. The osteoblasts were then permeabilized with 0.2% Triton-X 100 in PBS for 10 minutes. An aliquot of 80  $\mu$ L of 100 nM rhodamine phalloidin (Cytoskeleton, Inc.) was used for staining the actin filaments of the osteoblasts. The samples were visualized using confocal microscopy (Nikon A1 TIRF). Images from the confocal microscope at 4 hours were used to analyze surface area occupied by the osteoblasts using pixels in Adobe Photoshop and NIH ImageJ [22].

### **Osteoblast Adhesion Quantification**

Samples obtained from methods described in the co-culture system establishment section were washed with PBS ( $\times 2$ ). For osteoblast collection, trypsin, 600  $\mu$ L was added to the samples to de-attach the osteoblasts. FBS, 60  $\mu$ L, was added to trypsinized samples and mixed to cease the trypsinization. The 660  $\mu$ L trypsin/osteoblast solution was removed and added to a 1.5 mL centrifuge tube. The osteoblasts were centrifuged for 7 minutes at 1300 rpm. The pellet was resuspended with 20  $\mu$ L DMEM and then quantified using trypan blue and a hemocytometer.

## Bacteria Adhesion Quantification

Samples obtained from methods described in the co-culture system establishment section were washed with PBS ( $\times 2$ ). For bacteria collection, titanium samples from each time point were placed in individual capped-glass vials containing PBS. The supernatant from the osteoblast adhesion quantification section was removed and placed in respective bacteria glass vials with the titanium sample. Glass vials were capped and sonicated for 10 minutes to remove the bacteria. The bacteria were then plated, and CFUs were counted.

## Statistical Analysis

Statistical analysis was performed on measures of osteoblast and *S. aureus*. Student's t-test was performed to determine significant differences between the groups. The differences were considered statistically significant if  $p < 0.05$ .

## Results

### Osteoblast and *S. aureus* Attachment and Adhesion in the Low-Bacteria/Osteoblast (L-B) System

Osteoblast adhesion to the titanium surface is a requirement for successful osseointegration of the implant. In order to determine the efficacy of each sample, osteoblast on Ti surfaces were quantified at 30 minutes to determine initial attachment of bacteria and osteoblasts, and 4 hour time points, to determine adhesion, in co-culture conditions. Under L-B co-culture conditions at 30 minutes, the number of osteoblasts on the SA-CS-Ti surface ( $10,083 \pm 2,626$ ) were significantly higher than those on the SA-Ti ( $7,050 \pm 350$ ) and the UN-Ti ( $7,966 \pm 861$ ) (Figure 1-A). At the 4 hour time point, the UN-Ti and the SA-CS-Ti samples were significantly higher in osteoblast attachment compared to the SA-Ti (Figure 1-B). Analysis of the change in osteoblast attachment number from 30 minutes to 4 hours showed that the UN-Ti sample had a 2.6 fold increase, whereas the osteoblast number on the SA-Ti decreased by 0.75 fold from 30 minute to 4 hour. The SA-CS-Ti sample had an osteoblast number increased by 1.3 times from the 30 minute to the 4 hour time point.

Quantification of *S. aureus* on each Ti surface was also performed at the 30 minute and 4 hour time points. For both the 30 minute and the 4 hour samples, L-B co-culture conditions showed a similar pattern where the number of bacteria attached decreased from the UN-Ti to the SA-Ti, with the smallest number of bacteria on the SA-CS-Ti (Figure 1-A, B). The number of bacteria on the SA-CS-Ti ( $916 \pm 325$ ) were significant lower than that of the UN-Ti ( $4,933 \pm 2,589$ ) and the SA-Ti ( $2,136 \pm 274$ ) at the 4 hour time point. Analysis of the change in bacteria adhesion from 30 minutes to 4 hours showed that the UN-Ti and the SA-Ti samples had a 164 and 92 fold increase in bacteria, respectively, whereas the increase in bacteria attachment on the SA-CS-Ti surface was about 55 fold.

### Osteoblast and *S. aureus* Attachment and Adhesion in High-Bacteria/Osteoblast (H-B) system

Quantification of osteoblasts in H-B co-culture was obtained at 30 minute and 4 hour time points. At the 30 minute time point, the SA-CS-Ti sample had a significantly higher number of osteoblasts compared to both the UN-Ti and the SA-Ti (Figure 2-A). At the 4 hour time

point, the SA-Ti had a significantly lower osteoblast number compared to both the UN-Ti and SA-CS-Ti (Figure 2-B). Analysis of the change in osteoblast attachment from 30 minutes to 4 hours showed that the UN-Ti sample had a 1.96 fold increase, whereas for both the SA-Ti and SA-CS-Ti, the osteoblast number decreased.

Quantification of *S. aureus* in H-B co-culture was obtained at 30 minute and 4 hour time points. At the 30 minute time point, the SA-CS-Ti sample had a significantly lower number of bacteria than the UN-Ti and the SA-Ti (Figure 2-A). At the 4 hour time point, the SA-Ti had the greatest number of bacteria followed by the UN-Ti, while the SA-CS-Ti had the lowest number of bacteria attached (Figure 2-B).

### Scanning Electron Microscopy

For electron microscopy, Ti materials without osteoblasts and bacteria cells were observed to determine the topography of each sample (Figure 3). UN-Ti was smooth while both the SA-Ti and the SA-CS-Ti appeared rough. Using SEM, we also studied the interaction of osteoblast and bacteria in both L-B and H-B systems at the 30 minute and 4 hour time points. At the 30 minute time point, we expected the osteoblasts to remain round shaped in morphology as the osteoblasts are beginning to attach. At 4 hours, the osteoblasts attached and had begun to adhere to the surface and were expected to have a normal, polygonal morphology.

At 30 minutes in L-B conditions on the UN-Ti, osteoblasts remained rounded in morphology showing initial attachment with some osteoblasts displaying a polygonal morphology (Figure 4, A). Both the SA-Ti and the SA-CS-Ti samples at 30 minutes in L-B showed rounded osteoblast-like cell morphology (Figure 4, C and E, respectively). *S. aureus* was not readily observed at 30 minutes in the L-B conditions for each sample. At 30 minutes in H-B conditions, osteoblasts on the UN-Ti surface remained rounded in morphology, showing initial attachment (Figure 4, B). *S. aureus* was observed at a higher magnification on the UN-Ti samples and shown in Figure 4b and indicated by a red arrow. The SA-Ti sample at 30 minutes in the H-B conditions had osteoblasts in a polygonal morphology as well as rounded morphology, as the osteoblasts adapt to the rough surface topography (Figure 4, D). *S. aureus* was observed on the SA-Ti sample as shown in Figure 4d. Osteoblasts were rounded in morphology on the SA-CS-Ti samples in H-B conditions at 30 minutes, with some osteoblasts displaying polygonal morphology (Figure 4, F). *S. aureus* was not readily observed on the SA-CS-Ti sample or on the osteoblasts (Figure 4, f).

At the 4 hour time point, there were noticeable changes in osteoblast morphology as the osteoblasts began to adhere to the surface. At 4 hours in L-B conditions, osteoblasts on the UN-Ti surface were primarily polygonal with some rounded osteoblasts (Figure 5, A). *S. aureus* was readily observed both on the surface of the UN-Ti sample as well as on the osteoblasts (Figure 5, A). The SA-Ti samples at 4 hours in H-B showed osteoblasts in both polygonal and rounded morphology with no bacteria readily observed (Figure 5, C). The SA-CS-Ti sample at 4 hours in L-B showed osteoblasts in primarily polygonal morphology with no bacteria readily observed (Figure 5, E). In the H-B conditions at 4 hours, osteoblast behavior on the UN-Ti had osteoblast in both polygonal and rounded morphology (Figure 5, B). Significant interaction of *S. aureus* and osteoblast was observed at a higher

magnification on the UN-Ti sample (Figure 5, b). Osteoblast morphology on both the SA-Ti (Figure 5, D) and the SA-CS-Ti (Figure 5, F) samples had a significant amount of osteoblasts with polygonal morphology, with some osteoblasts rounded in morphology. In the SA-Ti group, *S. aureus* was observed on both the material and osteoblast surfaces (Figure 5, d). For the SA-CS-Ti, no *S. aureus* was found on the material surface and few bacteria were observed on the osteoblast surface (Figure 5, f).

### Confocal Microscope Preparation and Observation

Cytoskeletal osteoblast structure was observed using a confocal microscope after rhodium phalloidin staining to reveal the alteration in osteoblast morphology from 30 minutes to 4 hours. In the osteoblast single culture system, the majority of the osteoblasts began to have a spreading morphology on the UN-Ti surface (Figure 6-A1) at the 30 minute time point. However, when osteoblasts were in co-culture with *S. aureus*, the osteoblasts were observed to decrease in attachment, and a majority of the osteoblasts were in a rounded morphology instead of the spreading morphology (Figure 6-A2 and A3). For both modified Ti surfaces, morphology of the osteoblasts at the 30 minute time point were observed to be rounded with minimal spreading (Figure 6, B1-C3). The osteoblasts in the SA-Ti environment remained consistent in attachment and morphology despite co-culture conditions (Figure 6, B1-B3). Osteoblasts interacting with the SA-CS-Ti surface at 30 minutes remained rounded in morphology with minimal spreading (Figure 6, C1-C3). In the SA-CS-Ti co-culture conditions, the osteoblasts began to agglomerate as shown in Figure 6-C2 and C3.

Osteoblast spreading was clearly observed for each sample at the 4 hour time point. For the osteoblast only and H-B co-culture, a dense network of osteoblasts with a spreading morphology (elongated osteoblasts) were observed on UN-Ti samples, (Figure 7-A4 and A6, respectively). In the presence of L-B, however, the osteoblasts on the UN-Ti had a decreased density of spreading (Figure 7-A5). The rough SA-Ti sample had a low density of osteoblast spreading in all culture conditions (Figure 7, B4-B6). The SA-CS-Ti sample had a high level of osteoblast spreading and remained consistent in each culture condition at the 4 hour time point. Surface area calculations show that the osteoblasts on the SA-CS-Ti had the largest occupied surface area compared to the SA-Ti and UN-Ti in the both L-B (Figure 8-A) and H-B (Figure 8-B) system at 4 hours.

### Discussion

The biocompatibility of a material is closely related to cell/material interactions primarily influenced by the material's surface properties. For orthopedic implant materials, surface characteristics, such as the topography, play an essential part in osteoblast/material interaction. The quality of the first phase of cell-material interaction, consisting of cell attachment, adhesion and spreading, influences the cells' capacity to proliferate and to differentiate itself on contact with the implant. Using the co-culture systems in the presence of three different titanium samples with different surface properties, we investigated the interaction between osteoblast and *S. aureus* in a "race for the surface" scenario.

The co-culture system was developed to investigate and observe the behavior of osteoblast and bacteria to each Ti surface at the same time to simulate a race for the surface. The

purpose of both L-B and H-B co-culture systems was to mimic situations where infection can begin with a low or a high concentration of bacteria. A situation where a low concentration of bacteria can cause infection could be related to the contamination of implant materials by the patient's normal microflora. High bacteria concentrations can be introduced to the body in situations such as wounds seen in military combat [23–25]. We examined two co-culture systems to determine if the modified Ti material can be effective against different levels of microbial contamination and enhance osteoblast attachment to win the race for the surface.

In this study, the effect of bacteria level on osteoblast/Ti material interaction was evaluated with the two co-culture systems. Results showed that the presence of H-B had significant effect on osteoblast attachment, an essential component for osseointegration. At the 30 minute time point, osteoblast attachment was significantly higher on the SA-CS-Ti compared to the other two Ti samples, but the osteoblast number decreased significantly when the co-culture time increased to 4 hours (Figure 2-A, B). The L-B showed the highest statistically significant level of osteoblast attachment on the SA-CS-Ti at the 30 minute time point. Furthermore, the SA-CS-Ti and the UN-Ti samples had significantly higher osteoblast numbers than the rough SA-Ti at 4 hour (Figure 1-A, B).

To evaluate the potential of the Ti materials, it was important to look at the bacteria attachment between the 30 minute and 4 hour time points as well. Under L-B conditions, the SA-CS-Ti had lower attached bacteria at both the 30 minute and 4 hour time points than UN-Ti and SA-Ti samples (Figure 1-A, B). Results from the H-B system showed that the SA-CS-Ti had significantly fewer bacteria than UN-Ti at 30 minutes (Figure 1-A).

These results are consistent with the “race for the surface” hypothesis in which it is desired that the level of osteoblasts attachment is high and the level of bacteria attachment is low. The observed differences in the capability of osteoblast/bacteria adhesion to the Ti surfaces could be explained by the chitosan coating on the SA-CS-Ti. Chitosan is an antimicrobial agent with a mechanism of action that is postulated to be the binding of chitosan to teichoic acids, coupled with a potential extraction of membrane lipids (predominantly lipoteichoic acid) resulting in a sequence of events, ultimately leading to bacterial death [26–28]. Quantitative analysis showed that the L-B co-culture system at 30 minutes encouraged significantly higher osteoblast attachment to the SA-CS-Ti surface compared to the UN-Ti and the SA-Ti (Figure 1A and 1B). SEM and confocal microscope observations also showed that the osteoblasts have greater spreading morphology on the SA-CS-Ti (Figure 4E, 5E, and 7C-5). These quantitative and qualitative results of osteoblast adhesion indicate that the osteoblasts possess a greater surface area in the L-B system during the entire experimental period. Quantitative analysis showed that the H-B co-culture system at 30 minutes encouraged significantly higher osteoblast attachment to the SA-CS-Ti surface than the UN-Ti and the SA-Ti. At the 4 hour time point there was a significant decrease in osteoblast attachment on the SA-CS-Ti surface (Figure 2A and 2B). Although the number of attached osteoblasts decreased on the SA-CS-Ti, SEM and confocal observations showed that there is a greater quality in the adhesion of the osteoblasts compared to the UN-Ti (Figure 5F and 7C-6). Further analysis based on confocal images revealed that the surface area of the attached osteoblasts on the SA-CS-Ti was distinctly higher than that on the SA-Ti and UN-



TI (Figure 8). Research has demonstrated that enhancing the attachment function of osteoblast cells at the implant surface is likely to significantly decrease implant failure.[29] Another factor potentially leading to the decrease in osteoblast number on the SA-CS-Ti could be due to the fact that the antimicrobial properties of chitosan lead to bacteria death. A consequence of bacterial death is the release of bacterial toxins resulting in a decrease in osteoblast attachment. Future studies could focus on the gene and protein expressions of bacterial toxins and their effect on the adhesion behavior of osteoblasts on different Ti surfaces.

Material topography, as mentioned above, plays an essential role in osteoblast adhesion, a key factor for osseointegration, as well as bacteria adhesion. The co-culture system was aimed to simulate a “race for the surface” and SEM allowed for the observation of bacteria and osteoblast interaction as well as the effect of surface topography on osteoblast and bacteria adhesion behaviors. The SEM images showed that the three samples (UN-Ti, SA-Ti, and SA-CS-Ti) have differing surface topographies and surface characteristics. As reported in our earlier studies, the surface height variation significantly increased after the sulfuric acid treatment (SA-Ti) and the subsequent chitosan immobilization (SA-CS-Ti)[18]. The 1800× magnification was used in order to observe osteoblast behavior. *S. aureus* adhesion was observed at the 4600× magnification. The 30 minute time point was used to observe the initial osteoblast and bacterial attachment. Initial attachment was identified as the osteoblasts were still rounded in shape compared to the 4 hour time point where adhesion behavior, such as osteoblast spreading began to take place (Figure 4–5).

The quality of the osteoblast attachment (observed at 30 minutes), adhesion (observed at 4 hours) and spreading, influences the osteoblast’s ability to proliferate and to differentiate itself on contact with the implant. The SEM imaging at the 30 minute time point showed the behavior of osteoblasts that had just attached as they were still rounded. Each sample displayed a similar osteoblast morphology. At the 4 hour time point, osteoblast adhesion had occurred (Figure 5) with the osteoblasts appearing to have adhered to the SA-Ti and SA-CS-Ti more so than the UN-Ti samples based on how the cells adapted to the rough surface. At the 4 hour time point in L-B, the osteoblasts on the UN-Ti (Figure 4, A) were observed more rounded, as observed by the increased height of the osteoblasts, than the rough surfaces (Figure 4, C and D). This phenomenon could be explained by the mechanical adhesion of the osteoblasts to rougher surfaces on both SA-Ti and SA-CS-Ti, which could potentially lead to improved osseointegration. Moreover, while *S. aureus* was observed on both UN-Ti and SA-Ti, no bacteria could be observed on the surface of SA-CS-Ti, pointing to great potentials of SA-CS-Ti as novel osteogenic and anti-infective implant materials.

Confocal microscopy was used to view the cytoskeleton of the osteoblasts as the osteoblast begins to spread, another essential factor in osseointegration. At the 30 minute time point, all osteoblasts were bright red and rounded in morphology (Figure 6). At the 4 hour time point the osteoblasts began to spread (Figure 7). The confocal microscopic images showed a clear view of the osteoblast cytoskeleton. The osteoblast-only UN-Ti surfaces showed spreading of the osteoblasts, but the SA-Ti sample (Figure 7, B4) showed that osteoblasts have minimal spreading, and a majority of osteoblasts were still in a rounded morphology.

Osteoblasts on SA-CS-Ti (Figure 7, C4-C6) showed spreading morphology in all the culture conditions.

## Conclusions

The long-term goal of this research was to combine two surface modifying techniques, sulfuric acid treatment and chitosan immobilization, to address the implant-related infections. In this study, we introduced two co-culture systems in testing anti-infective efficacy of Ti materials in the presence of both osteoblasts and bacteria. The quantitative and qualitative results showed that the incorporation of chitosan on an implant surface greatly encouraged osteoblast adhesion behaviors (including cell initial attachment, adhesion, and spreading) while significantly decreasing bacteria attachment simultaneously. These results also encourage our future research in further testing the “race for the surface” hypothesis and exploring related mechanisms underlying the effect of bacterial concentration on osteoblast adhesion mediated signals, such as osteoblast adhesins and specific infection markers. This work has shown the potential of the chitosan immobilization techniques to be used in future implant design to improve osseointegration and decrease implant related infections.

## Acknowledgements

Research reported in this publication was supported by the National Institutes of Health under Award Number R21AR065625. The content is solely the responsibility of the authors and does not necessarily represent the official views of the National Institutes of Health. We wish to acknowledge the help from Ms. Kelly Graber in the Imaging Core at Sanford Research for her help and guidance with confocal microscopy.

## References

1. Rupp F, Scheideler L, Olshanska N, de Wild M, Wieland M, Geis-Gerstorfer J. Enhancing surface free energy and hydrophilicity through chemical modification of microstructured titanium implant surfaces. *J Biomed Mater Res A*. 2006; 76:323–334. [PubMed: 16270344]
2. Le Guehenec L, Lopez-Heredia MA, Enkel B, Weiss P, Amouriq Y, Layrolle P. Osteoblastic cell behaviour on different titanium implant surfaces. *Acta Biomater*. 2008; 4:535–543. [PubMed: 18226985]
3. Gahlert M, Gudehus T, Eichhorn S, Steinhauser E, Kniha H, Erhardt W. Biomechanical and histomorphometric comparison between zirconia implants with varying surface textures and a titanium implant in the maxilla of miniature pigs. *Clin Oral Implants Res*. 2007; 18:662–668. [PubMed: 17608736]
4. Gittens RA, McLachlan T, Olivares-Navarrete R, Cai Y, Berner S, Tannenbaum R, Schwartz Z, Sandhage KH, Boyan BD. The effects of combined micron-/submicron-scale surface roughness and nanoscale features on cell proliferation and differentiation. *Biomaterials*. 2011; 32:3395–3403. [PubMed: 21310480]
5. Wu Y, Zitelli JP, TenHuisen KS, Yu X, Libera MR. Differential response of Staphylococci and osteoblasts to varying titanium surface roughness. *Biomaterials*. 2011; 32:951–960. [PubMed: 20974493]
6. Le Guehenec L, Soueidan A, Layrolle P, Amouriq Y. Surface treatments of titanium dental implants for rapid osseointegration. *Dent Mater*. 2007; 23:844–854. [PubMed: 16904738]
7. Cooper LF, Masuda T, Yliheikkila PK, Felton DA. Generalizations regarding the process and phenomenon of osseointegration. Part II. In vitro studies. *Int J Oral Maxillofac Implants*. 1998; 13:163–174. [PubMed: 9581401]
8. Li Y, Lee IS, Cui FZ, Choi SH. The biocompatibility of nanostructured calcium phosphate coated on micro-arc oxidized titanium. *Biomaterials*. 2008; 29:2025–2032. [PubMed: 18276003]

9. Rosa MB, Albrektsson T, Francischone CE, Schwartz Filho HO, Wennerberg A. The influence of surface treatment on the implant roughness pattern. *Journal of applied oral science : revista FOB*. 2012; 20:550–555. [PubMed: 23138742]
10. Burgers R, Gerlach T, Hahnel S, Schwarz F, Handel G, Gosau M. In vivo and in vitro biofilm formation on two different titanium implant surfaces. *Clin Oral Implants Res*. 2010; 21:156–164. [PubMed: 19912269]
11. Molin S, Tolker-Nielsen T. Gene transfer occurs with enhanced efficiency in biofilms and induces enhanced stabilisation of the biofilm structure. *Curr Opin Biotechnol*. 2003; 14:255–261. [PubMed: 12849777]
12. WHO. Antimicrobial resistance: global report on surveillance 2014. Geneva World Health Organization; 2014. 2014.
13. Shi Z, Neoh KG, Kang ET, Poh C, Wang W. Bacterial adhesion and osteoblast function on titanium with surface-grafted chitosan and immobilized RGD peptide. *J Biomed Mater Res A*. 2008; 86:865–872. [PubMed: 18041731]
14. Amoroso PF, Adams RJ, Waters MG, Williams DW. Titanium surface modification and its effect on the adherence of *Porphyromonas gingivalis*: an in vitro study. *Clin Oral Implants Res*. 2006; 17:633–637. [PubMed: 17092220]
15. Zhao L, Chu PK, Zhang Y, Wu Z. Antibacterial coatings on titanium implants. *J Biomed Mater Res B Appl Biomater*. 2009; 91:470–480. [PubMed: 19637369]
16. Yuan Y, Chesnutt BM, Wright L, Haggard WO, Bumgardner JD. Mechanical property, degradation rate, and bone cell growth of chitosan coated titanium influenced by degree of deacetylation of chitosan. *J Biomed Mater Res B Appl Biomater*. 2008; 86:245–252. [PubMed: 18161778]
17. Quirynen M, van der Mei HC, Bollen CM, Schotte A, Marechal M, Doornbusch GI, Naert I, Busscher HJ, van Steenberghe D. An in vivo study of the influence of the surface roughness of implants on the microbiology of supra- and subgingival plaque. *J Dent Res*. 1993; 72:1304–1309. [PubMed: 8395545]
18. Ghimire N, Luo J, Tang R, Sun Y, Deng Y. Novel anti-infective activities of chitosan immobilized titanium surface with enhanced osteogenic properties. *Colloids and Surfaces B: Biointerfaces*. 2014; 122:126–133. [PubMed: 25033432]
19. Gristina AG, Naylor P, Myrvik Q. Infections from biomaterials and implants: a race for the surface. *Med Prog Technol*. 1988; 14:205–224. [PubMed: 2978593]
20. Liu C, Bayer A, Cosgrove SE, Daum RS, Fridkin SK, Gorwitz RJ, Kaplan SL, Karchmer AW, Levine DP, Murray BE, M JR, Talan DA, Chambers HF. A Infectious Diseases Society of, Clinical practice guidelines by the infectious diseases society of america for the treatment of methicillin-resistant *Staphylococcus aureus* infections in adults and children. *Clin Infect Dis*. 2011; 52:e18–55. [PubMed: 21208910]
21. Cramton SE, Gerke C, Schnell NF, Nichols WW, Gotz F. The intercellular adhesion (ica) locus is present in *Staphylococcus aureus* and is required for biofilm formation. *Infect Immun*. 1999; 67:5427–5433. [PubMed: 10496925]
22. Agle CC, Velloso CP, Lazarus NR, Harridge SD. An image analysis method for the precise selection and quantitation of fluorescently labeled cellular constituents: application to the measurement of human muscle cells in culture. *J Histochem Cytochem*. 2012; 60:428–438. [PubMed: 22511600]
23. Burns TC, Stinner DJ, Mack AW, Potter BK, Beer R, Eckel TT, Possley DR, Beltran MJ, Hayda RA, Andersen RC, Keeling JJ, Frisch HM, Murray CK, Wenke JC, Ficke JR, Hsu JR. C. Skeletal Trauma Research, Microbiology and injury characteristics in severe open tibia fractures from combat. *The journal of trauma and acute care surgery*. 2012; 72:1062–1067. [PubMed: 22491628]
24. Arens S, Schlegel U, Printzen G, Ziegler WJ, Perren SM, Hansis M. Influence of materials for fixation implants on local infection. An experimental study of steel versus titanium DCP in rabbits. *J Bone Joint Surg Br*. 1996; 78:647–651. [PubMed: 8682836]
25. Wenke JC, Guelcher SA. Dual delivery of an antibiotic and a growth factor addresses both the microbiological and biological challenges of contaminated bone fractures. *Expert Opin Drug Deliv*. 2011; 8:1555–1569. [PubMed: 22017669]

26. Neoh KG, Hu X, Zheng D, Kang ET. Balancing osteoblast functions and bacterial adhesion on functionalized titanium surfaces. *Biomaterials*. 2012; 33:2813–2822. [PubMed: 22257725]
27. Rabea EI, Badawy ME, Stevens CV, Smagghe G, Steurbaut W. Chitosan as antimicrobial agent: applications and mode of action. *Biomacromolecules*. 2003; 4:1457–1465. [PubMed: 14606868]
28. Kong M, Chen XG, Xing K, Park HJ. Antimicrobial properties of chitosan and mode of action: a state of the art review. *Int J Food Microbiol*. 2010; 144:51–63. [PubMed: 20951455]
29. Masuda H, Iwasaki H, Kawamoto A, Akimaru H, Ishikawa M, Ii M, Shizuno T, Sato A, Ito R, Horii M, Ishida H, Kato S, Asahara T. Development of serum-free quality and quantity control culture of colony-forming endothelial progenitor cell for vasculogenesis. *Stem cells translational medicine*. 2012; 1:160–171. [PubMed: 23197763]

### Highlights

- Titanium surface was immobilized with chitosan:SA-CS-Ti.
- Two bacteria/osteoblastco-culture systems were proposed and established.
- The co-culture systems were used for testing the race for the surface behavior.
- The SA-CS-Ti decreased bacteria and increased osteoblast adhesions simultaneously.

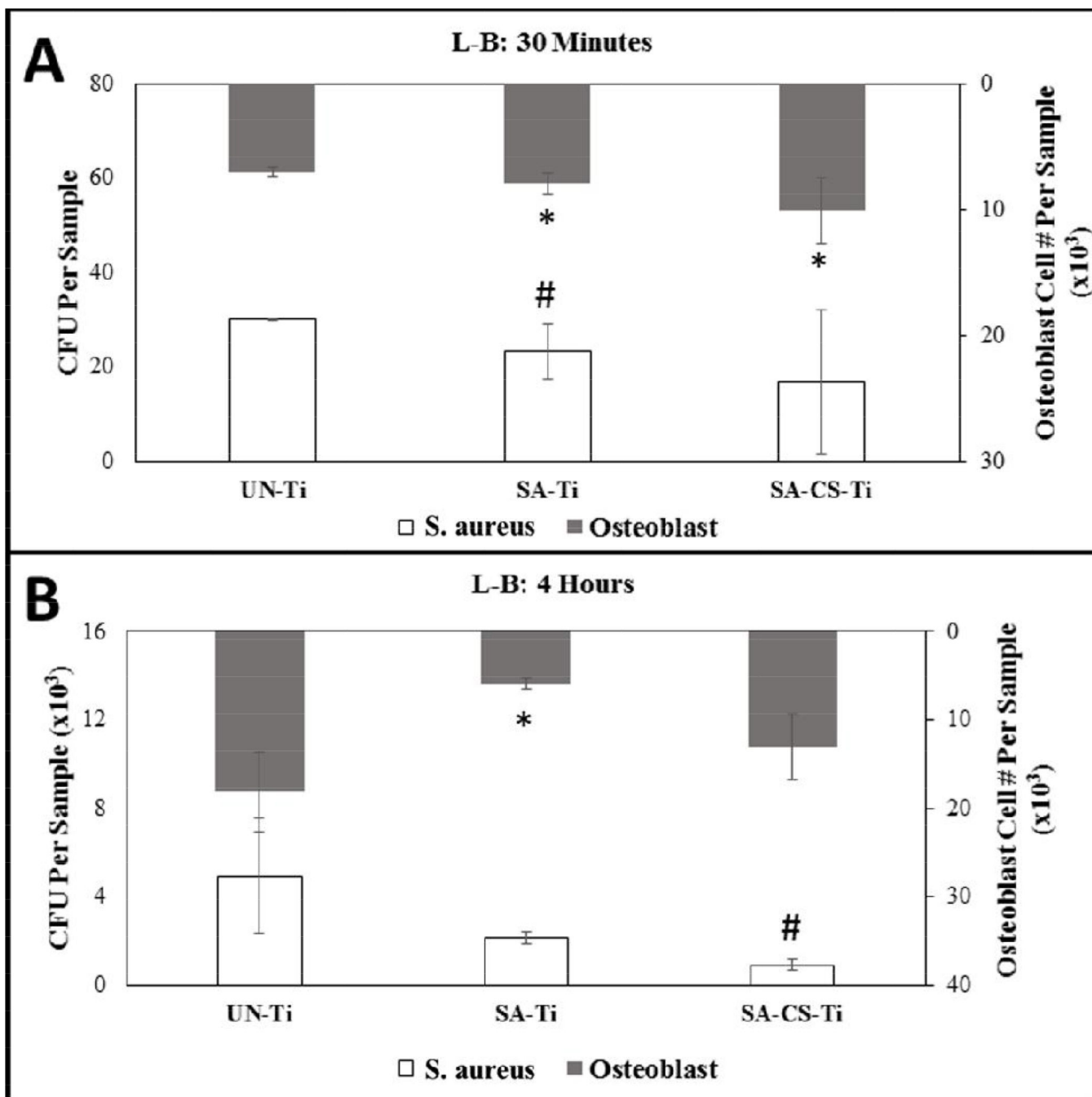


**Figure 1.**

L-B co-culture graphs showing quantitation of osteoblast and bacteria at 30 minute (A) and 4 hour time (B) points. The results showed that the UN-Ti sample increased the greatest in both osteoblast attachment and bacteria over the 30 minute and 4 hour time points. The SA-CS-Ti had increased osteoblast attachment and had the lowest bacteria attachment over the 30 minute and the 4 hour time points. \* and # ( $p < 0.05$ ) denotes the statistical significance from the UN-Ti group.

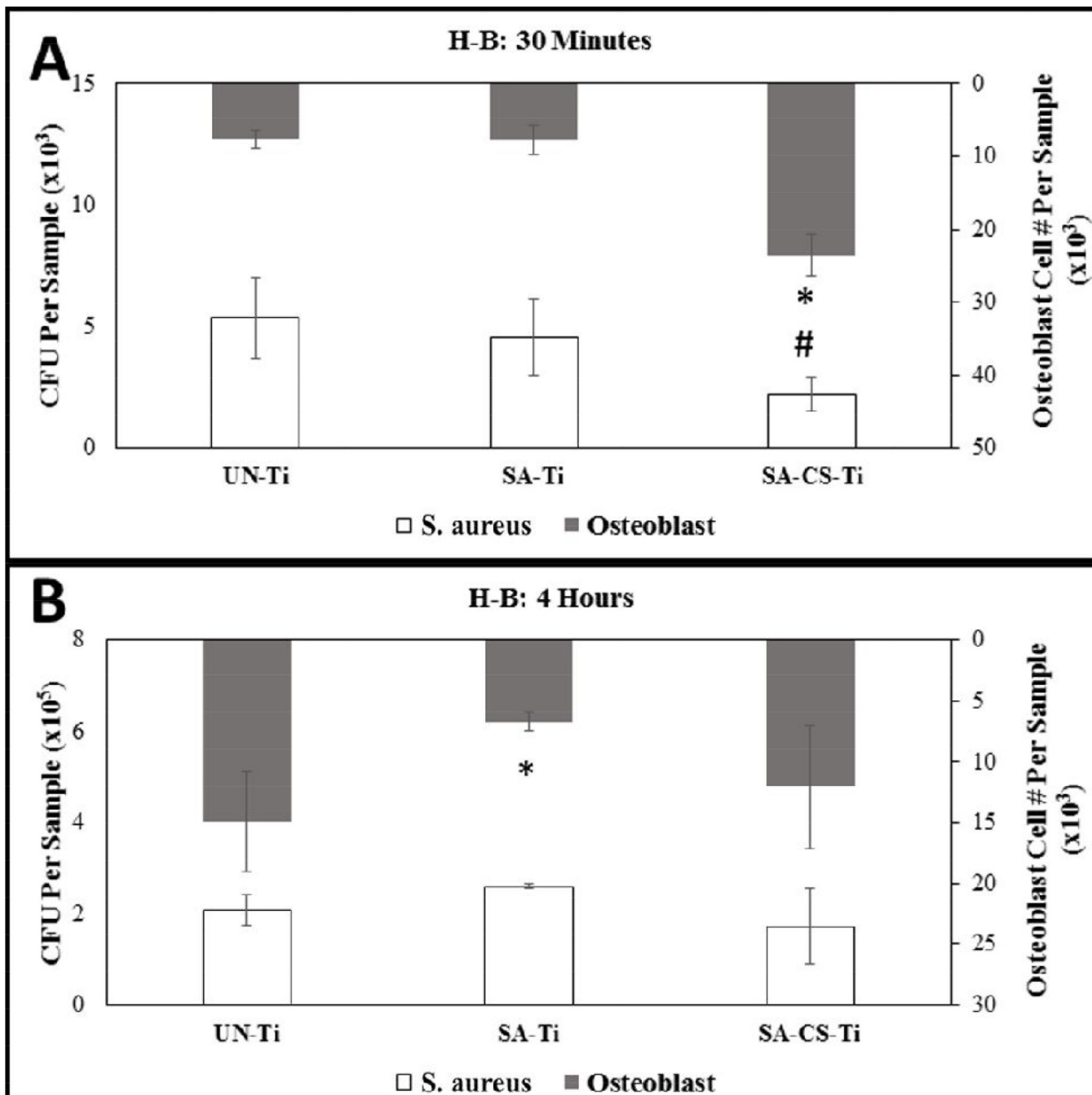


**Figure 2.**

H-B Co-culture graphs showing quantitation of osteoblast and bacteria at 30 minute (A) and 4 hour time (B) points. The SA-CS-Ti had decreased the number of osteoblast attached, yet had the lowest number of bacteria attachment over 30 minute and 4 hour time points. Statistical significance from the UN-Ti group is denoted by \* and # ( $p < 0.05$ ).

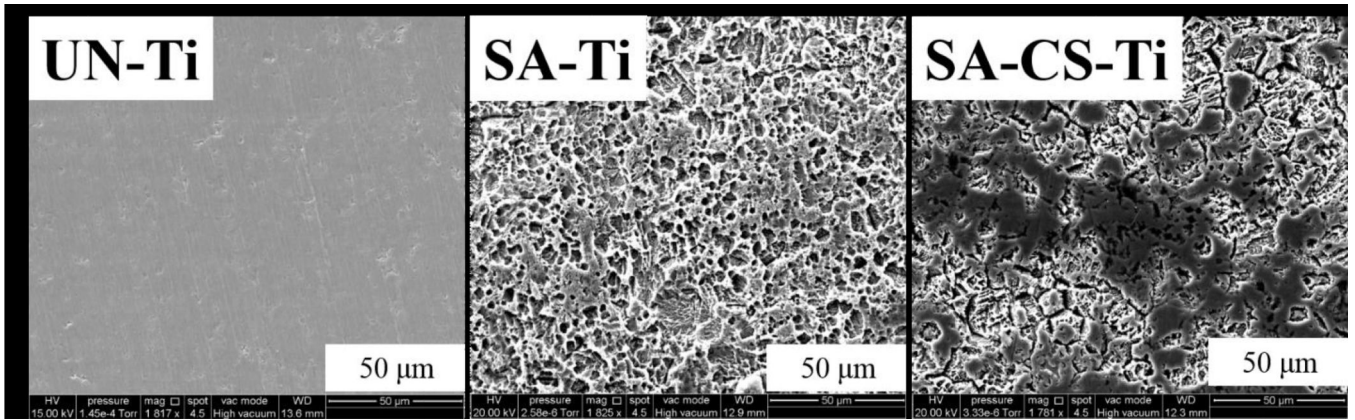


**Figure 3.** SEM observations of different Ti materials. UN-Ti is smooth, SA-Ti shows rough, porous topography, and the SA-CS-Ti shows roughness with chitosan on the surface.



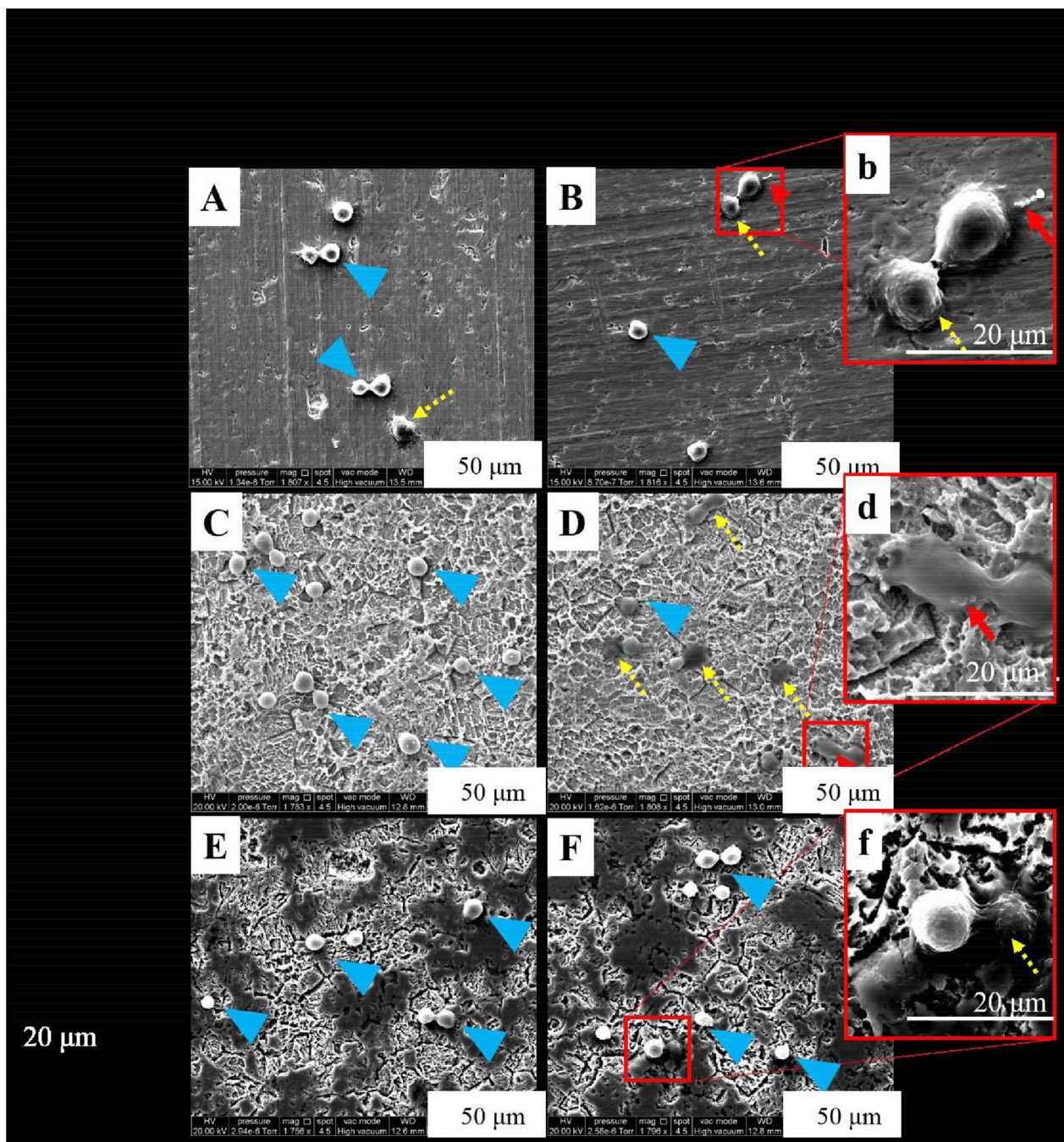


**Figure 4.**

SEM observations of osteoblast and *S. aureus* behavior on different Ti materials at 30 minutes. SEM micrographs of osteoblasts in L-B conditions on UN- Ti (A), SA-Ti (C) and SA-CS-Ti (E) showed rounded morphology as the osteoblasts attached to the surface. SEM micrographs of osteoblast in H-B conditions on UN-Ti (B, b), SA-Ti (D, d), and SA-CS-Ti (F, f) showed osteoblasts in a rounded morphology but with more osteoblasts adhering to the surface as they showed a polygonal morphology. Blue arrows indicate osteoblast initial attachment, yellow dashed arrows indicate cell adhesion, and red arrows indicate bacteria

colony observations with a magnified view in the insert image. For fig A-F magnification=1800×, and for inserts b, d, f, magnification=4600× magnified.

Author Manuscript

Author Manuscript

Author Manuscript

Author Manuscript

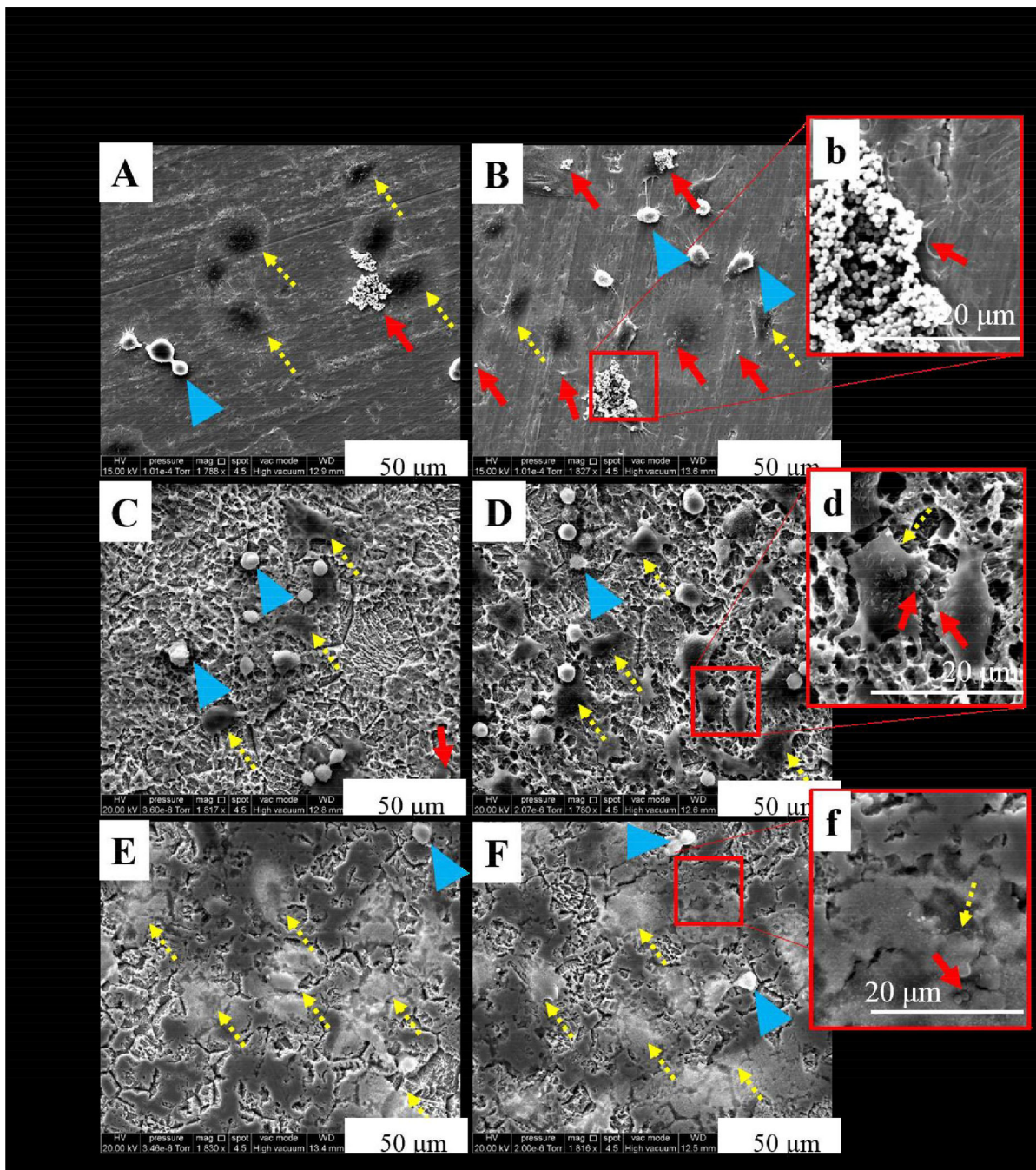


**Figure 5.**

SEM observations of osteoblast and *S. aureus* behavior on different Ti materials at 4 hours. SEM micrographs of osteoblasts in L-B conditions on UN- Ti (A), SA-Ti (C) and SA-CS-Ti (E) showed polygonal morphology as the osteoblasts adhere to the surfaces; however, rounded morphology is still observed. SEM micrographs of osteoblast in H-B conditions on UN-Ti (B, b), SA-Ti (D, d), and SA-CS-Ti (F, f) show osteoblasts in a polygonal morphology. Blue arrows indicate osteoblast initial attachment, yellow dashed arrows indicate cell adhesion, and red arrows indicate bacteria colony observations with a magnified

view in the insert image. For fig A-F magnification=1800×, and for inserts b, d, f, magnification=4600×.

Author Manuscript

Author Manuscript

Author Manuscript

Author Manuscript

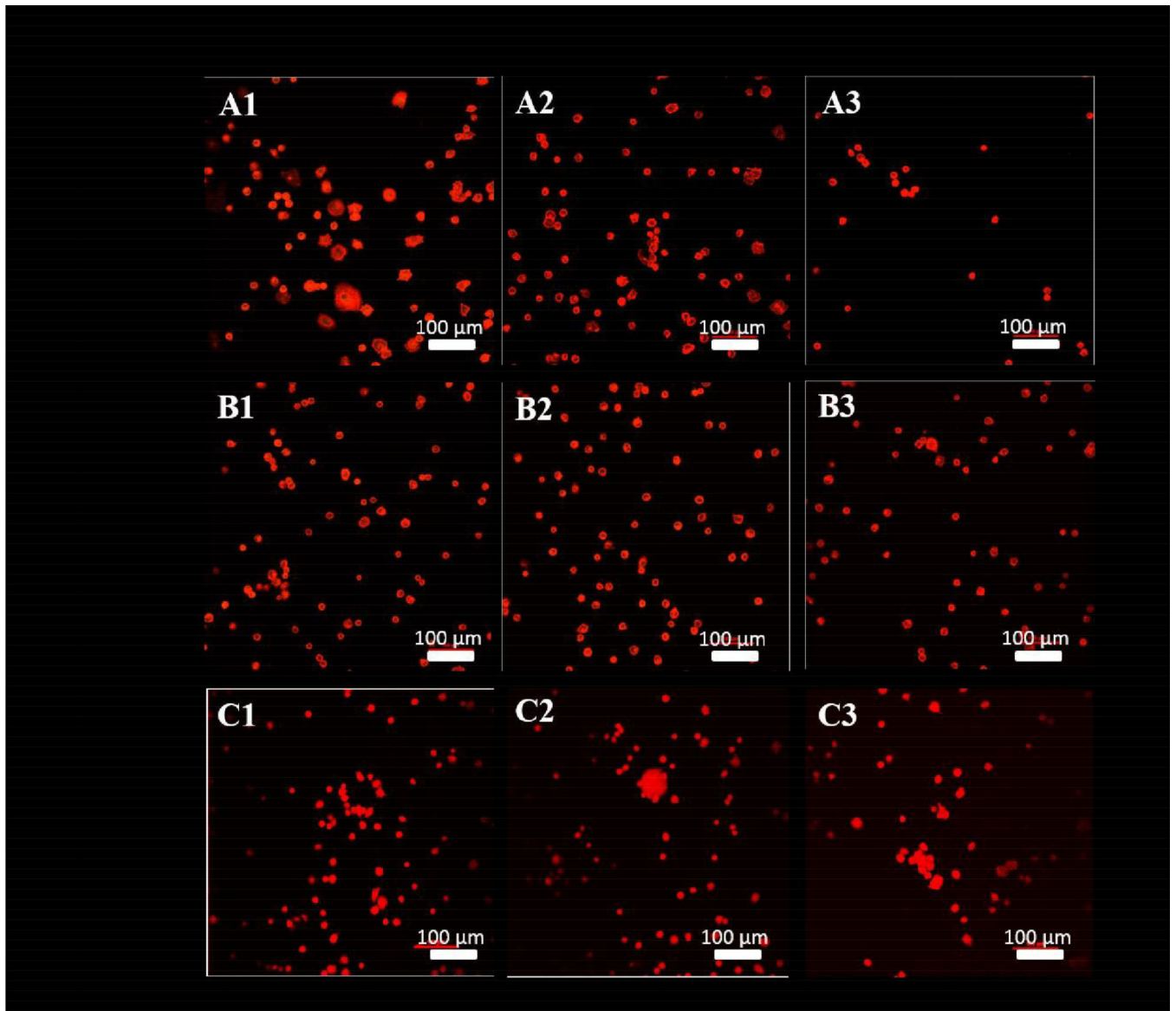


**Figure 6.** Cytoskeleton visualized with confocal microscopy using rhodium phalloidin dye at 30 minutes. UN-Ti (A1-A3), SA-Ti (B1-B3) and SA-CS-Ti (C1-C3). Osteoblasts are in the process of attaching to the surface, so their morphology is expected to be rounded as they have not had time to adhere and spread.

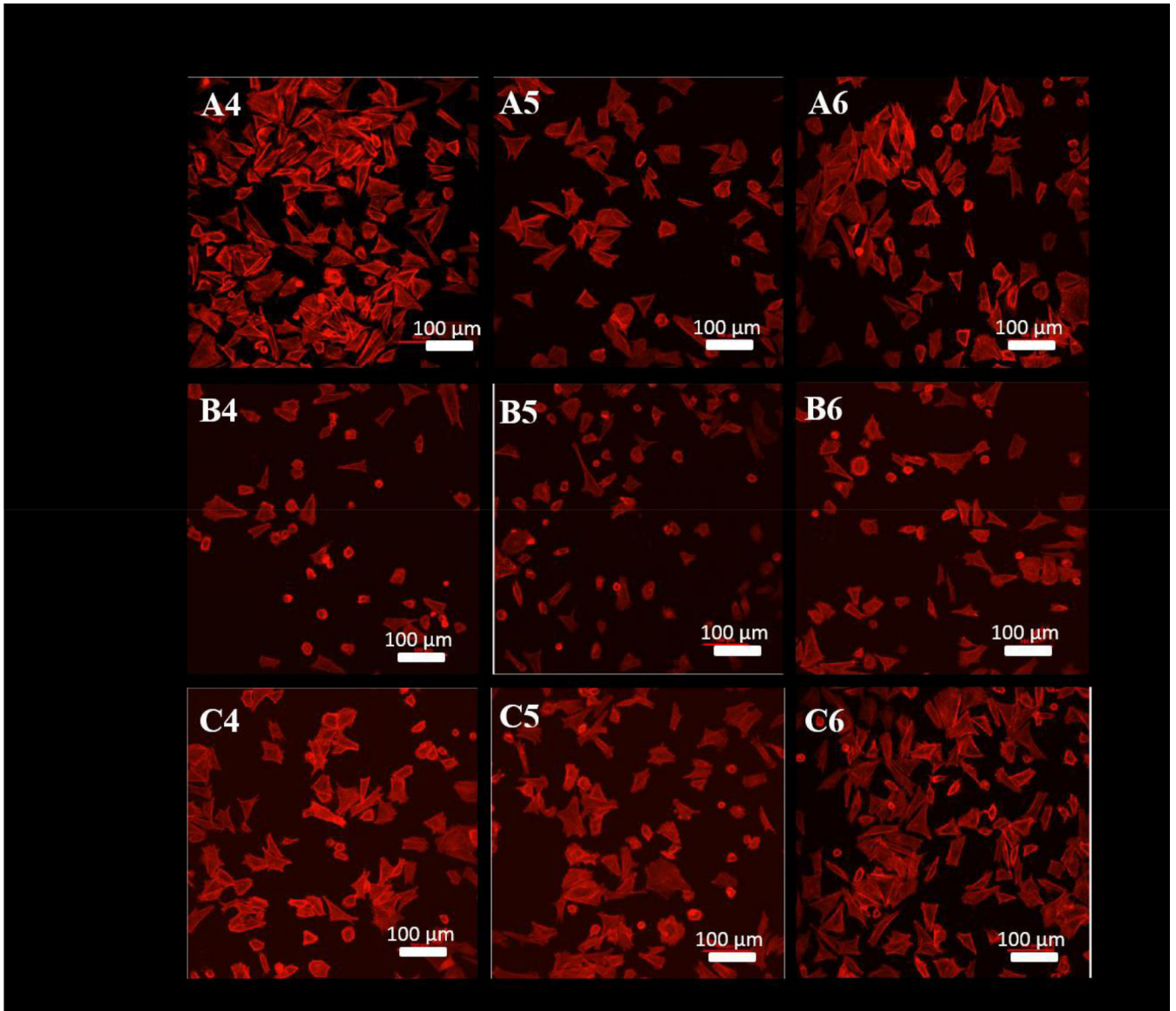


**Figure 7.** Cytoskeleton visualized with confocal microscopy using rhodium phalloidin dye at 4 hours. UN-Ti (A4-A6), SA-Ti (B4-B6) and SA-CS-Ti (C4-C6). Osteoblast spreading is indicated by the red stained osteoblasts that are elongated on each surface. The rounded morphology of the osteoblasts show that osteoblasts have either recently attached or have not spread yet.

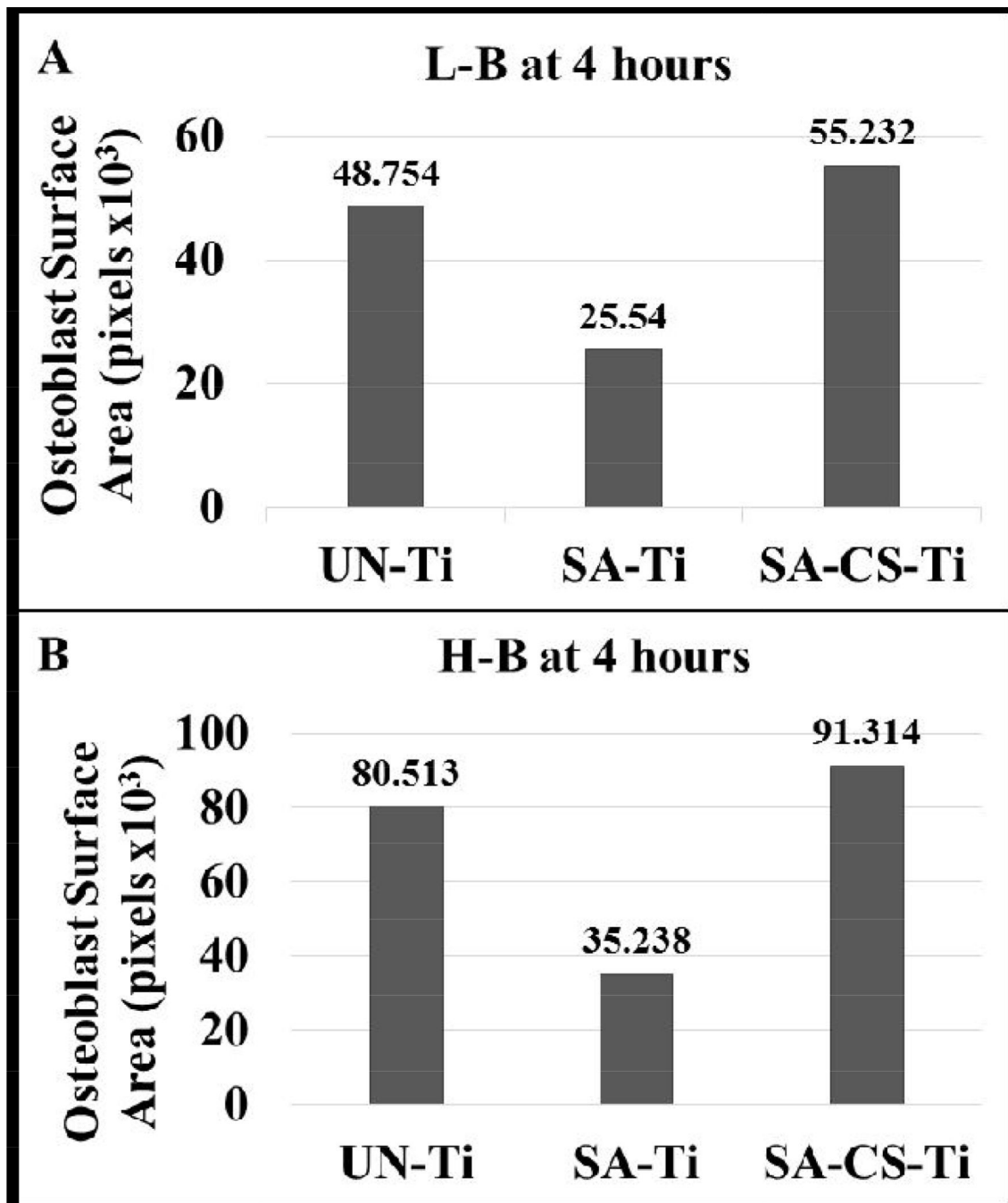


**Figure 8.**

Total cell surface area calculation for osteoblast attached on different Ti materials. A representation of total cell surface area was determined from the corresponding images in figure 7. The results showed that the osteoblasts on the SA-CS-Ti had the largest surface area in both the L-B and H-B system at 4 hours.